



# EXPLORING TRANSIENT INSTATIONARITIES OF MECHANICAL LOAD IN THE OPERATION OF WASTEWATER PUMPS

Florian BROKHAUSEN<sup>1</sup>, Paul Uwe THAMSEN<sup>2</sup>,

<sup>1</sup> Corresponding Author. Chair of Fluid System Dynamics, Faculty of Mechanical Engineering and Transport Systems, Technische Universität Berlin. Straße des 17. Juni 135, 10623 Berlin. E-mail: florian.brokhausen@tu-berlin.de

<sup>2</sup> Chair of Fluid System Dynamics, Faculty of Mechanical Engineering and Transport Systems, Technische Universität Berlin. Straße des 17. Juni 135, 10623 Berlin. E-mail: paul-uwe.thamsen@tu-berlin.de

## ABSTRACT

The operation of pumps in wastewater conditions is objected to complex failure modes due to the heterogeneous nature of wastewater as a medium. The main operational challenge is the clogging of the pump due to nonwoven wipes accumulating in the impeller. To investigate the operation of wastewater pumps and emulate clogging phenomena, a standardized testing procedure, in which dusters are mixed with clear water to emulate the characteristics of the suspended nonwoven wipes in real wastewater is employed. In this paper, the joint analysis of mechanical and hydraulic measurements provides deeper insights into the characteristic phenomena that constitute clogging events in wastewater pumps. The mechanical data analyzed entails the torque and rotational speed, synchronized with the hydraulic measurement of the pump head and flow. With baseline clear water measurements and constrained wastewater operation tests, salient signatures in mechanical and hydraulic data are attributable to the influence of the wastewater medium and clogging events. The volatile and persistent clogging states of a pump induce transient instationarities in the mechanical load, especially reflected in the high-frequency oscillation of torque in the form of harmonic distortion. This is demonstrated via 19 standardized tests performed on 10 pumps with semi-open two-channel impellers.

**Keywords:** Clogging Characterization, Frequency Domain Analysis, Instationary Mechanical Load, Wastewater Pumps

## NOMENCLATURE

$BPF$	$[Hz]$	Blade Passing Frequency
$DFT$	$[-]$	Discrete Fourier Transform
$H$	$[m]$	Head
$M$	$[Nm]$	Torque
$Q$	$[m^3/h]$	Flow
$RF$	$[Hz]$	Rotational Frequency
$VFD$	$[-]$	Variable Frequency Drive

$m_w$	$[g]$	Weight
$\eta$	$[%]$	Efficiency

## Subscripts and Superscripts

$CW$	Clear Water
------	-------------

## 1. INTRODUCTION

Pumps utilized in wastewater management are crucial components for the transportation and processing of wastewater, which often contains a complex mixture of suspended solids, organic matter, and chemical substances. These pumps are specifically designed to handle such diverse and potentially abrasive materials, ensuring continuous fluid movement. [1] A significant operational challenge, however, is the phenomenon of clogging, predominantly caused by nonwoven wipes. These materials, commonly found in domestic wastewater, have a tendency to accumulate within the pump's impeller, resulting in obstructions that can impair pump performance and, in extreme cases, lead to complete system failure [2].

The consequences of clogging are reductions in flow rate or pump head, increased energy consumption, and amplified mechanical stress and wear. Further, the growing frequency of extreme weather events, in combination with the ongoing trend of urbanization, places additional stress on wastewater infrastructure, increasing the urgency of maintaining the operational integrity of pumps. As such, it is imperative that the design of wastewater pumps incorporates features that enhance resistance to clogging, thereby ensuring long-term efficiency.

While previous research has identified nonwoven wipes as a primary contributor to clogging, much of the existing literature has been limited to theoretical models or simulations. Empirical investigations into the interaction between wastewater impellers and fibrous materials remain scarce. This gap underscores the need for more experimental studies

that provide concrete insights into the mechanisms of clogging and its deduced influence on a pump's operating conditions.

Hence this study provides new and valuable insights into the impact of clogging and general wastewater operating conditions on the mechanical power driving the wastewater pump. To deduce these influences, the chair of Fluid System Dynamics at the Technische Universität Berlin employs a designated test rig to emulate wastewater conditions in a controlled environment. This test rig enables the investigation of a pump's susceptibility to clogging and provides valuable insights into the detailed mechanisms constituting diverse clogging phenomena.

In this work, the designated test rig is leveraged to gain insights into the influence of wastewater operating conditions and clogging events on the mechanical powertrain, namely the torque and rotational speed. In total, 19 tests are carried out on 10 different pumps equipped with a range of different semi-open two-channel impeller designs, objected to varying degrees of emulated contamination. In these tests, the hydraulic performance in terms of flow and pump head are tracked as well as the mechanical load in terms of rotational speed and torque. Besides the analysis in the value domain, the torque is additionally analyzed in the frequency domain to observe the oscillatory behavior and how this is impacted by clogging of the pump's impeller.

## 2. RELATED WORK

The research area of investigating and characterizing clogging in wastewater pumps and its influence on common process measurements is scarce. Especially so when focusing on experimental works with realistic testing scenarios.

The work of Kallweit [3] presents a baseline for the change of parameters under clogging conditions. Here, the author presents experiments with fixed, constant, artificial clogging on an axial impeller's blades and analyzes the implications. In particular, the authors analyze pressure pulsations in the frequency domain which are shown to substantially deviate for clogging conditions of the tested impeller.

However, a focus on the changes in mechanical load in wastewater pumps with respect to clogging events has not yet been presented. Many studies do employ rotational speed and torque measurements or calculations, but exclusively with the aim to determine mechanical power leveraged for pump efficiency investigations [4, 5]. These investigations do not, however, focus on the implications of clogging but instead on the optimization design aspects for the reduction of power consumption. As the majority of related work on wastewater pumps, these studies also mainly present a simulation of the setup, with only reduced experiment capacities for verification purposes.

The work of Barrio et al.[6] does consider frequency domain analysis of the torque of a pump in

terms of the blade passing frequency amplitude of torque. However, these reports are only based on simulation results. Further, the impeller is designed for clear water operation.

Consequently, to the best of the author's knowledge, this is the first work to investigate mechanical load and particularly torque, in realistic wastewater conditions to this depth and show the large oscillations in the torque harmonics induced by clogging events. This work falls in line with previous efforts in characterizing signal patterns for clogging in wastewater pumps carried out at the Technische Universität Berlin [7, 8, 9, 10].

## 3. MATERIALS AND METHODS

### 3.1. Test Rig Setup

The chair of Fluid System Dynamics at the Technische Universität Berlin operates a designated test rig for standardized testing of wastewater pumps.

**Test Rig and Procedure.** Figure 1 shows the test rig used to carry out the standardized wastewater tests. The test rig is composed of two  $3.5\text{ m}^3$  tanks that are connected through looped pipes, integrating the pump under test. The various valves enable the configuration of different circuits to move the water. For the standardized testing, water is pumped in a circle from and to the wastewater tank. The test medium is artificial wastewater consisting of clear water mixed with dusters. These dusters have a size of  $22 \times 33\text{ cm}$  with a fabric weight of  $60\text{ g/m}^2$ . They have been found to most closely reproduce the clogging phenomena observed in wastewater pumps in the field induced by nonwoven wipes [2, 11]. The standardized test is called the *long-time functional performance test*, where the artificial wastewater is pumped in a loop for the duration of an hour. The operation of the motor, and thus the pump, is facilitated with a variable frequency drive (VFD). The VFD is set to maintain a constant speed of rotation.

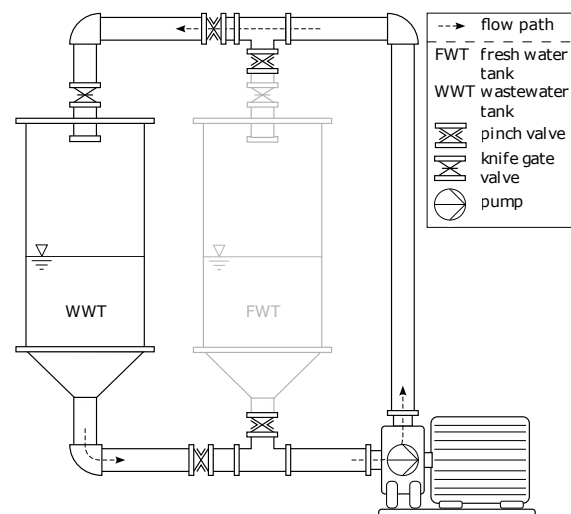


**Figure 1. Schematic of the test rig and the flow paths.**

After a test, the pump is opened to retrieve the dusters clogged in the impeller of the pump. With this, the weight ratio of all dusters introduced in the test and the ones remaining clogged in the pump at the end of the test is determined. This weight ratio assumes a value of 1 when all introduced dusters are clogged inside the pump at the end of the test. Oppositely, a weight ratio of 0 implies that all dusters have been continuously pumped without being accumulated in the pump at the end of the test. This test can be repeated for three different so-called *contamination classes*. These modify the number of dusters introduced in the test in steps of 25, 50, or 100 dusters per cubic meter of water.

For each long-time functional performance test of a pump, the so-called *degree of long-time functionality* ( $D_{LTF}$ ) is calculated according to the following equation [7]:

$$D_{LTF} = \frac{1}{2} \cdot \frac{\bar{\eta}}{\eta_{CW}} + \frac{1}{2} \cdot \frac{m_{w,total} - m_{w,pump}}{m_{w,total}}, \quad (1)$$

where  $\bar{\eta}$  is the average efficiency of the test,  $\eta_{CW}$  is the efficiency of the pump in clear water operation and  $m_{w,-}$  are the weights of the total introduced dusters in the test and the weight of dusters remaining in the pump at the end of the test.

In addition to the long-time functional performance tests, a clear water reference measurement of 30 s is recorded for each operating point of the pump under test. The obtained clear water values serve as a reference for the changes in the hydraulic, mechanical, and electric characteristics which are induced in the long-time functional performance tests due to wastewater operating conditions and potential clogging.

**Sensor Setup.** In order to analyze the operation of the pump under wastewater conditions, several measurements are carried out to determine important performance metrics. The differential pressure is measured between the inlet and outlet of the pump, according to DIN EN ISO 9906 [12]. The flow is determined with an inductive flow meter. These measurements enable the calculation of the pump head. All measurements are recorded with a sampling frequency of 1 Hz.

For the purposes of this study, the test rig is equipped with an additional torque transducer. The torque transducer is the measurement flange T40B by HBK. This enables not only the measurement of the torque but the rotational speed as well. The torque is measured with a high accuracy of a maximum 0.03 %. As the previously defined metrics, the rotational speed is recorded with a frequency of 1 Hz. Since the torque is analyzed in the frequency domain as well, the sampling frequency is set to 1000 Hz.

### 3.2. Pumps under Test

In total, a number of 10 pumps are tested for the purposes of this investigation. For these 10

pumps, 19 tests are performed with varying contamination classes. Generally, with any pump, the testing starts at the lowest contamination class and increases gradually across the denoted classes. A pump is only tested with the next higher contamination class if the respective  $D_{LTF}$  value is above 0.4, as otherwise the pump will only exhibit even more severe clogging with no added insights. For the purpose of this study, the  $D_{LTF}$  is merely a means to formalize the experimentation and will not be discussed and analyzed further.

The pumps under test are all equipped with semi-open two-channel impellers. The impellers vary in their leading edge configuration in terms of thickness and streamlines. The pumps P1 to P3 exhibit increasing degrees of cutback on the leading edge, i.e. decreasing how far the leading edge reaches into the inlet of the casing. The impellers of pumps P4 to P6 are modifications of P4 with increased leading edge thickness. Finally, pumps P7 to P10 are equipped with impellers observing connected leading edges of varied thickness. All impellers exhibit a diameter of 310 mm. The volute casing is the same for all tests, as is the motor, VFD, and sensor setup. The in- and outlet of the casing are DN200 and DN150, respectively.

In all tests of the different impellers, the rotational speed of the motor is set to  $1450 \text{ min}^{-1}$  via the VFD.

### 3.3. Frequency Domain Transfer

**Fourier transform.** The frequency domain transfer is set up in a similar fashion as in the work of Brokhausen et al. [10]. The process will be briefly described here as well.

The frequency domain transfer is executed via a discrete Fourier transform (DFT) since the data it is applied to is characterized as real-valued and digitized. The result of this transform is a complex amplitude spectrum over the frequencies. These complex amplitudes are converted to real, absolute values and are converted back to their original value domain for ease of interpretation. This is implemented as follows (adapted from [13, p. 61]):

$$A_M = \frac{2 \cdot |A_c|}{N}, \quad (2)$$

where  $A_M$  are the amplitudes in the original value domain,  $A_c$  are the complex amplitudes, and  $N$  is the number of data points the DFT was applied to.

**Windowed DFT.** The frequency transform is applied in a windowed fashion. The window is shifted by a certain number of samples across the data, where a DFT is carried out per window. This enables the resolution of the amplitudes over time. The number of samples, the window is shifted by therefore defines the resolution in time. The frequency resolution is defined by the size of the window. The smallest frequency that can be resolved is determined by

the division of the sampling frequency by the window size.

The extracted windows of data need to be further conditioned. When extracting a subsection of data, the constituent waveforms are cut at a point that is unequal to their period. This leads to the detection of amplitudes for frequencies, which in reality do not exist in the data. This phenomenon is called spectral leakage. It is countered by applying a window function to each window. In this study, the Hamming window is used. The Hamming window represents a bell curve with reduced kurtosis and is formulated as follows [14]:

$$w(n) = 0.54 - 0.46 \cdot \cos\left(\frac{2\pi n}{N-1}\right), \quad (3)$$

with  $0 \leq n \leq N-1$

where  $N$  represents the number of samples in a window. The window function essentially dampens the edges of the windows to reduce their influence in terms of spectral leakage. With the application of this function, however, the resulting amplitudes of the DFT are of course altered. In order to counter this and be able to still interpret the amplitude spectrum in the original value domain, an amplitude correction factor needs to be applied. The correction factor is calculated by Equation 4 [15, p. 212]:

$$CF = \frac{N}{\sum_{n=0}^{N-1} w(n)}, \quad (4)$$

where, again,  $N$  is the size of the window. The resulting amplitudes are all multiplied by this correction factor.

**Implementation details.** The frequency domain transfer via the windowed discrete Fourier transform is executed with a window size of 1000 samples. As mentioned, the sampling frequency of the torque measurement is 1000 Hz, making the window one second long. Moreover, this results in a frequency resolution of 1 Hz. This is a sufficient resolution in frequency as the frequencies of interest are not as close to one another as to necessitate a sub-Hertz resolution. This is demonstrated in the subsequent chapter.

With this setup, the maximum frequency that can be identified is 500 Hz, which is far enough for the harmonics being observed in the measurements, as demonstrated later on in the results. Lastly, the number of samples the window is shifted by is set to 500, i.e. 0.5 s. This ensures a sufficient resolution in time.

### 3.4. Definition of Harmonics

The reason for the frequency domain analysis is to be able to identify and trace harmonics in the torque signal. The expected and observed harmonics originate due to the inherent periodic nature of the mechanic rotation. Therefore, the main base fre-

quency is the rotational frequency (RF). One specific additional frequency of interest is the so-called blade passing frequency (BPF), i.e. the frequency with which the blades of the pump's impeller rotate. Naturally, this depends on the number of blades and manifests as the product of the latter and the rotational frequency. As all pumps in this study employ two-channel impellers, i.e. possessing two distinct blades, their blade passing frequency is twice the rotational frequency.

The notion of harmonics manifests as integer multiples of these base frequencies. Table 1 shows the frequencies of interest evaluated in this study. The table shows both, the exact frequency as well as the binned frequency at which the respective harmonic will be identified due to the frequency resolution of 1 Hz.

The table shows another important peculiarity. In this case, the second harmonic of the rotational frequency is synonymous with the blade passing frequency, as both manifest at twice the rotational frequency. Therefore, only the odd harmonics of the rotational frequency are regarded.

Additionally, as the third harmonic of the rotational frequency showcases, the exact frequency of occurrence can be located in the center of two integer frequencies. In this case, due to instationarities in the operation, the frequency bin the harmonic manifests in can change between the two values. In order to account for cases like this and general variance in the exact occurrence of the harmonic amplitude peaks, these are identified as the most prominent peak within a range of  $\pm 5$  Hz around the theoretically defined center frequency.

In the remainder of the paper, these harmonics may be referred to with a shortened descriptor in the format of  $(X \cdot)RF$  and  $(X \cdot)BPF$  to represent the  $X^{th}$  harmonic.

### 3.5. Analysis Strategy

**Aggregate analysis in the time domain.** As a first step, the focal metrics of this study are analyzed separately and time-independent. For this, the distribution of the assumed values of the rotational speed and torque are presented and analyzed per long-time functional performance test. The values are reported in a normalized fashion by being divided by the respective clear water value at the set operating point. Therefore, the spread of the deviation of torque and

**Table 1. Non-exhaustive list of frequencies of interest**

Description	Exact Value	Binned Value
Rotational Frequency	24.16 Hz	24 Hz
Third Harmonic of RF	72.5 Hz	73 Hz
Fifth Harmonic of RF	120.83 Hz	121 Hz
Blade Passing Frequency	48.3 Hz	48 Hz
Second Harmonic of BPF	96.6 Hz	97 Hz

speed due to wastewater operating conditions can be deduced.

#### Aggregate analysis in the frequency domain.

The second part of the aggregate analysis is focused on the averaged harmonic amplitudes for all tests. All amplitudes for the frequencies of interest from Table 1 are averaged over time for each test, resulting in a metric per harmonic per test. These amplitudes are normalized by the amplitude of the respective clear water operation as well, therefore representing the relative increase or decrease in amplitude. This analysis gives a first insight into the impact of wastewater operation and clogging on the harmonic amplitudes in the torque.

**Integrated time and frequency domain analysis.** In order to analyze the hydraulic and mechanical time-related metrics jointly with the frequency domain metrics, the latter are resolved in time as well via the reported windowing approach. Therefore, the head, flow, and torque, as well as the amplitudes of the harmonics of the torque can be reported in a synchronized fashion on a shared time base. This is done for demonstrative tests which are chosen based on the aggregate analyses to represent the prevalent findings.

## 4. RESULTS

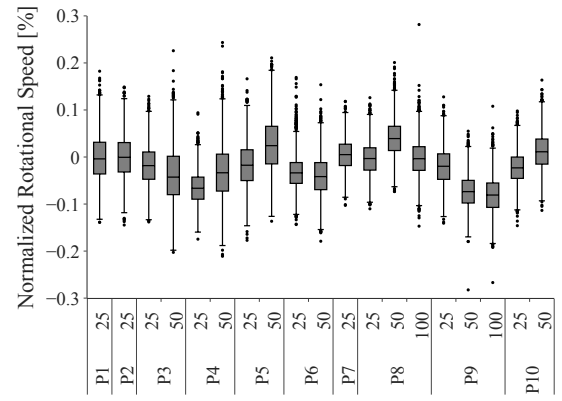
### 4.1. Aggregate Analysis in Time Domain

**Rotational speed.** For the aggregate analysis of the distribution of values of the rotational speed, the normalized, relative values are shown as individual box plots per test in Figure 2a. These values can be interpreted as a percentage increase or decrease in rotational speed compared to the set clear water speed. The x-axis shows the labels for the respective pump as well as the contamination class employed in the test.

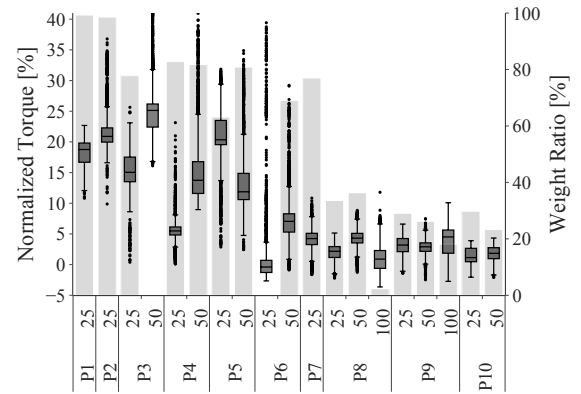
As can be seen by the very small range of the y-axis, the rotational speed does not vary a lot during the long-time functional performance test with artificial wastewater. The largest deviation from the set rotational speed of any test is below  $\pm 0.3\%$ . The median rotational speed of all tests even falls within  $\pm 0.1\%$  of the set speed.

**Torque.** The distribution of assumed torque values during the test is represented in the same way as the rotational speed, as boxplots of normalized values in Figure 2b. This figure additionally shows the weight ratio of each test as a bar, mapped to the right-sided y-axis. The weight ratio signifies the amount of dusters that accumulated in the pump at the end of the respective test.

In contrast to the rotational speed, the torque shows a lot more variation, with maximum values exceeding 40 % increase of the needed torque for clear water operation. Further, many more outliers can be observed, as seen by the amount of markers beyond the whiskers of the boxplots. This represents the occurrence of sudden spikes and peaks in the torque induced by the dusters' interference with the impeller.



(a) Rotational Speed.



(b) Torque.

**Figure 2. Boxplots for all tests showing the distribution of the rotational speed (a) and torque (b), normalized by their respective clear water operation values. Plot (b) additionally shows the weight ratio as bars mapped to the second, right-sided y-axis.**

The overlaid weight ratio shows the relation between the severity of clogging of the pump and the attributed increase in the necessary torque. The tests where more severe clogging occurs, i.e. observing a higher weight ratio, also show a higher median of the torque and tend to generally exhibit more variance with more prominent peak values. Moreover, this tendency is also reversely true: tests, where few dusters are accumulated in the pump, tend to show a median closer to zero and less variance.

**Discussion.** The analysis of the rotational speed shows how well the VFD regulates and controls the delivered speed. Despite the demonstrated increases in torque, the set rotational speed can be very accurately maintained by the control.

The deviations in the operating conditions present due to the clogging of the pump mechanically only reflect in the supplied torque. This is supported by the observed tendency that the median and variance are increased when there are more dusters clogged in the pump. There are some exemptions,

like the test with contamination class 25 for pump P7. Here, 77 % of the dusters remain clogged in the pump, but the median torque is only increased by about 3.5 % compared to clear water operation.

Another obvious exemption to these observations is the test of pump P6 with contamination class 25. Here, no clogging occurred at the end of the test. The median torque in this test also exhibits the lowest value out of all tests, which falls in line with the overall tendency. However, the variance of torque from this test is among the largest of all tests. This can be attributed to transient clogging states occurring over the duration of the test. Since the weight ratio only describes the state at the end of the test, any short-lived and transient clogging events are not reflected in this metric. Therefore, analyses need to be carried out over time as well.

#### 4.2. Aggregate Analysis in Frequency Domain

For the aggregate analysis in the frequency domain, Figure 3 shows the relative change of the average amplitudes for the frequencies of interest for each test. The change is reported relative to the amplitudes of the harmonics in clear water operation.

For the rotational frequency, there are no discernible tendencies to be observed. Only for the tests of pumps P1, P2, and P3, there is a notable increase in amplitude to be seen of up to 300 % in the case of pump P1. For the remainder of the tests, the amplitudes for the RF do not increase or decrease drastically and show no apparent pattern. The amplitudes of the third harmonic of the rotational frequency show a more unified response in that for all tests but one, there is an increase in the amplitude. For tests P1-25, P5-50, and P6-50, there is a particularly strong gain in amplitude. These observations are similar for the fifth harmonic of the RF.

An entirely different effect can be seen for the blade passing frequency, where the amplitude actually decreases for all but one test. The exemption being the test P1-25, which increasingly manifests as an outlier to the overall tendencies. Lastly, the second harmonic of the BPF increases for all performed tests. The highest increase for any harmonic is observed for test P4-50 with an increase of 317 %.

**Discussion** In the aggregate analysis in the frequency domain, some harmonics of the rotational and blade passing frequencies show tendencies to change in common ways when operating in wastewater conditions. This is further supported when revisiting the weight ratios of the individual tests reported in Fig. 2b. In the tests for pumps P1 through P7, with the exemption of test P6-25, the severity of clogging in terms of the weight ratio is a lot more prominent than for the remainder of the tests. This is reflected in the averaged relative change of the harmonic amplitudes. Here, the increase in the 2-BPF is especially prominent. The harmonic amplitudes of 3-RF also mainly show a larger increase than in the tests with

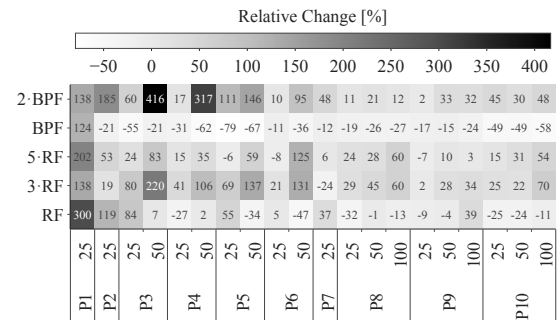


**Figure 3. Relative increase of amplitudes at harmonic frequencies for all tests.**

less severe clogging. This holds true as well for the observed decrease in magnitude of the BPF.

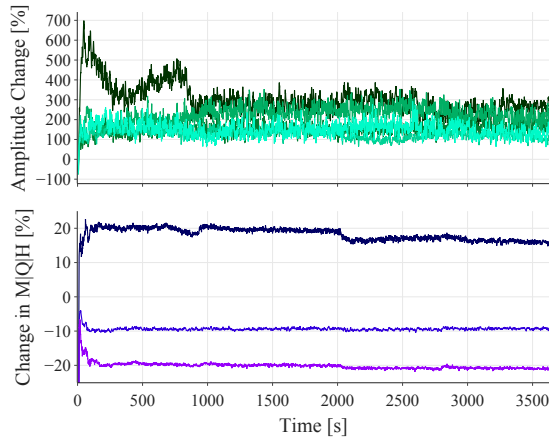
#### 4.3. Integrated Time and Frequency Domain Analysis

The synchronized analysis of time and frequency domain components of the torque and the hydraulic performance metrics is facilitated by Figure 4. The figure shows the data for three exemplary tests, namely the test of pump P1 at the lowest contamination class 25 as well as tests of pumps P4 and P6 for the medium and lowest contamination classes, respectively.

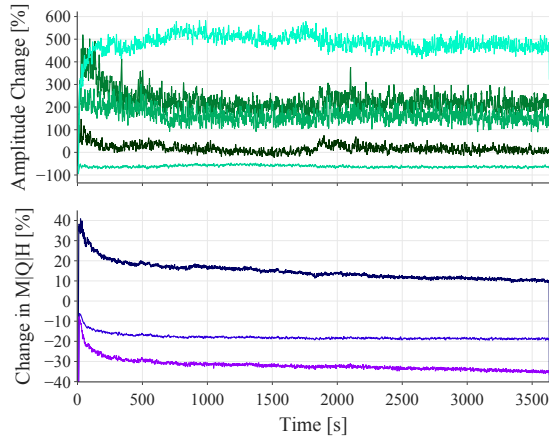
Each of the subplots is assembled the same way: the respective top plot shows the five harmonics of interest. Here, the amplitudes are normalized by their clear water operation values to get the relative changes in amplitude induced by the wastewater conditions. The bottom plots show the head, flow, and torque data, normalized by their respective clear water operation values as well and transformed to a percentage. All values can directly be interpreted as percentage-wise increases or decreases.

In Figure 4a, it can be seen that especially the amplitude of the rotational frequency increases drastically during the first 1000 s of the test, with relative increases of up to nearly 700 %. Additionally, all other harmonics observe increased amplitudes as well, with increases between 100 and 300 %. The overall level of the torque increases by 20 percent at the start of the test and drops to about a 15 % increase at the 2000 s mark. In contrast, the flow and head drop to a continuously lower level over the whole duration of the test, with respective losses of 10 % in flow and 20 % in head.

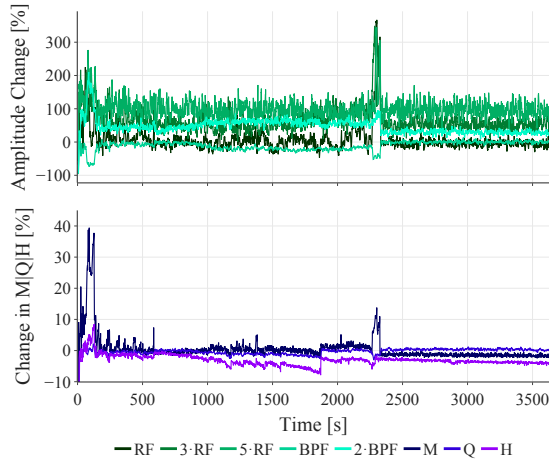
The test in Figure 4b exhibits very different trends. Here, the second harmonic of the BPF is the most prominent harmonic with increases of up to 580 %. The rotational frequency shows no elevated amplitude levels while its third and fifth harmonic increase around 200 % on average, the latter peaking at as much as 520 % increase at the beginning of the test. In contrast, the amplitude of the BPF shows continuously lower levels than in clear water operation with a drop of 60 to 70 %. Concurrently, the



(a) P1-25.



(b) P4-50.



(c) P6-25.

**Figure 4. Harmonic and hydraulic metrics over time for three different tests. The respective top plot shows the relative difference in harmonic amplitudes. The bottom plots show the relative difference in head, flow, and torque. The joint legend is located in (c).**

hydraulic performance metrics decrease from the beginning of the test, with the flow dropping to a continuously lower level of around 80 % of its clear wa-

ter reference. The head drops most prominently at the beginning as well, but then keeps slowly declining to a final value of 65 % of its clear water value. The magnitude of the torque again develops contrarily with increases of 40 % at the start and a continuous slow decline from this peak over the duration. The torque is still increased by about 10 % at the end of the test.

Lastly, the third test, reported in Figure 4c, shows rather inconspicuous harmonic levels most of the time. The same holds true for the hydraulic metrics and the overall torque level. However, there are two distinct events, at the beginning of the test and between 2250 and 2350 s, where the torque values increase drastically for a short duration. These events are reflected in the harmonics as well, where for both events the amplitude of the BPF drops below its clear water levels and the other harmonics show increased amplitudes.

**Discussion** The first two presented tests P1-25 and P4-50 both represent tests where clogging of the pump's impeller occurs from the start of the test. The final clogging accounts for 99 and 82 % respectively for the two tests. The state of clogging of the impeller is depicted in Figure 5.

The test P1-25 is the previously identified outlier from the overall observable harmonics trends in the data. This is also true when regarding the harmonics in a time-resolved manner, as all harmonics show a considerable increase due to severe clogging.

Test P4-50 features even more severe clogging, with, despite the smaller weight ratio, an overall higher weight of dusters remaining clogged in the impeller. This is especially reflected in the hydraulic performance as the head and flow decrease extensively. In the frequency domain, the harmonics show representative patterns as discovered to be prevalent in the aggregate analysis. The BPF is continuously smaller than in clear water operation while its second harmonic is highly increased. The increased torque at the beginning of the test is especially reflected in the third and fifth harmonic of the RF.

In the last test, P6-25, there was no clogged material inside the pump at the end of the test. Over most of the test duration, the pump is only very minorly clogged as observed during the test via a borescope. This minor clogging is reflected in the harmonics of the torque, especially through the increased levels of the third and fifth harmonic of the RF. The salient event after 2250 seconds, where the torque and its harmonics suddenly spike and then revert to their original levels again after about 100 seconds represents an event where more material is spontaneously accumulating in the impeller. Subsequently, all clogged material evacuates from the impeller and it stays clog-free until the end of the test. This presents the imprint of self-cleansing mechanisms as often observed in wastewater pumps [8] onto the required torque and its harmonics.





(a) P1-25.

(b) P4-50.

**Figure 5. Accumulated clogging after the respective test.**

## 5. CONCLUSION

The work presents insights from 19 standardized functional performance tests in realistic wastewater operating conditions for a total of 10 different wastewater pumps with semi-open two-channel impellers. The focus of the investigation lies on the mechanical load and clogging-induced instationarities in it. These are demonstrated in the value as well as frequency domain of the torque signal. In particular, clogging of the impeller was shown to lead to increased required torque levels as well as large increases in torque oscillation. The latter manifests as amplitude increases of harmonic frequencies of the rotational and blade passing frequencies with transient, relative increases of more than 600 %.

In future work, the aim is to project these torque deviations onto electrical power and current measurements within the variable frequency drive. This will mostly be achievable for the value domain, the application of frequency domain analyses, however, will presumably show different characteristics.

## REFERENCES

- [1] Von Sperling, M., 2007, *Wastewater characteristics, treatment and disposal*, IWA publishing.
- [2] Pöhler, M., 2020, *Experimentelle Entwicklung eines standardisierten Abnahmeverfahrens für Abwasserpumpen*, Mensch und Buch Verlag.
- [3] Kallweit, S., 1994, *Untersuchungen zur Erstellung wissensbasierter Fehlerdiagnosesysteme für Kreislumpen*, Technische Universität Berlin (Germany).
- [4] Caruso, F., and Meskell, C., 2021, "Effect of the axial gap on the energy consumption of a single-blade wastewater pump", *Proceedings of the Institution of Mechanical Engineers, Part A: Journal of Power and Energy*, Vol. 235.
- [5] Keays, J., and Meskell, C., 2006, "A Study of the Behaviour of a Single-Bladed Waste-Water Pump", *Proceedings of the Institution of Mechanical Engineers, Part E: Journal of Process Mechanical Engineering*, Vol. 220.
- [6] Barrio, R., Blanco, E., Parrondo, J., González, J., and Fernández, J., 2008, "The Effect of Impeller Cutback on the Fluid-Dynamic Pulsations and Load at the Blade-Passing Frequency in a Centrifugal Pump", *Journal of Fluids Engineering*, Vol. 130 (11).
- [7] Beck, D., Holzbauer, Y., and Thamsen, P. U., 2021, "Different Clogging Behavior of Wastewater Pumps", *Fluids Engineering Division Summer Meeting*, American Society of Mechanical Engineers.
- [8] Beck, D., Brokhausen, F., and Thamsen, P. U., 2022, "Time-Resolved Measurements for the Detection of Clogging Mechanisms", *Fluids Engineering Division Summer Meeting*, American Society of Mechanical Engineers.
- [9] Brokhausen, F., Herfurth, E., Beck, D., and Thamsen, P., 2023, "Exploring characteristics of time-resolved signals in the operation of wastewater pumps", *European Conference on Turbomachinery Fluid Dynamics and Thermodynamics*.
- [10] Brokhausen, F., Rost, L. M., and Thamsen, P. U., 2024, "Frequency Domain Analysis of Transient Discharge Pressure Harmonics for Clogging Detection in Wastewater Pumps", *Fluids Engineering Division Summer Meeting*, American Society of Mechanical Engineers.
- [11] Mitchell, R.-L., Gunkel, M., Waschniewski, J., and Thamsen, P. U., 2020, "Nonwoven Wet Wipes Can Be Hazardous Substances in Wastewater Systems—Evidences from a Field Measurement Campaign in Berlin, Germany", *Frontiers in Water-Energy-Nexus—Nature-Based Solutions, Advanced Technologies and Best Practices for Environmental Sustainability*.
- [12] DIN EN ISO 9906, 2012, "Rotodynamic Pumps—Hydraulic Performance Acceptance Tests—Grades 1, 2 and 3", .
- [13] Lyons, R. G., 2004, *Understanding Digital Signal Processing (2nd Edition)*, Prentice Hall PTR, USA.
- [14] Blackman, R. B., and Tukey, J. W., 1958, "The measurement of power spectra from the point of view of communications engineering—Part I", *Bell System Technical Journal*, Vol. 37.
- [15] Brandt, A., 2023, *Noise and vibration analysis: signal analysis and experimental procedures*, John Wiley & Sons.